

# Role of defects in improving electrical and optical properties of solution-processed transparent conducting Al-doped ZnO thin films



Thesis submitted in partial fulfillment  
for the Award of Degree

**Doctor of Philosophy**

by

*Anurag Kumar*

DEPARTMENT OF CERAMIC ENGINEERING  
INDIAN INSTITUTE OF TECHNOLOGY  
(BANARAS HINDU UNIVERSITY)  
VARANASI – 221005  
INDIA

Roll No. 17031003

2022

## **CERTIFICATE**

It is certified that the work contained in the thesis titled “**Role of defects in improving electrical and optical properties of solution-processed transparent conducting Al-doped ZnO thin films**” by **ANURAG KUMAR** has been carried out under my supervision and that this work has not been submitted elsewhere for a degree.

It is further certified that the student has fulfilled all the requirements of Comprehensive examination, Candidacy and SOTA for the award of Ph.D. Degree.



**Dr. Mohammad Imteyaz Ahmad**  
(Supervisor)  
Assistant Professor  
Department of Ceramic Engineering,  
IIT (BHU) Varanasi

## DECLARATION BY THE CANDIDATE

I, **Anurag Kumar**, certify that the work embodied in this thesis is my own bona fide work and carried out by me under the supervision of **Dr. Mohammad Imteyaz Ahmad, Assistant Professor** for a period of 5 years and 2 months from **July, 2017 to October, 2022**, at the **Department of Ceramic Engineering, Indian Institute of Technology (BHU), Varanasi**. The matter embodied in this Ph.D thesis has not been submitted for the award of any other degree/diploma. I declare that I have faithfully acknowledged and given credits to the research workers wherever their works have been cited in my work in this thesis. I further declare that I have not willfully copied any other's work, paragraphs, text, data, results, etc., reported in journals, books, magazines, reports dissertations, theses, etc., or available at websites and have not included them in this thesis and have not cited as my own work.

Date:

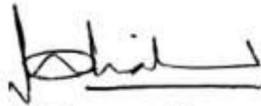


Place: Varanasi

(Anurag Kumar)

## CERTIFICATE BY THE SUPERVISOR

It is certified that the above statement made by the candidate is correct to the best of our knowledge.



**Dr. Mohammad Imteyaz Ahmad**  
(Supervisor)  
Assistant Professor  
Department of Ceramic Engineering  
IIT (BHU) Varanasi



**Prof. V K Singh**  
(Head of Department)  
Department of Ceramic Engineering  
IIT (BHU) Varanasi

Department of Ceramic Engineering  
सिरामिक अभियान्त्रिकी विभाग  
Indian Institute of Technology (B.H.U.)  
भारतीय प्रौद्योगिकी संस्थान (कां०हि०वि०वि०)  
Varanasi-221005/ वाराणसी-221005

## **COPYRIGHT TRANSFER CERTIFICATE**

Title of the Thesis: **Role of defects in improving electrical and optical properties of solution-processed transparent conducting Al-doped ZnO thin films.**

Name of the Candidate: **Anurag Kumar**

### **Copyright Transfer**

The undersigned hereby assigns to the Institute of Technology (Banaras Hindu University) Varanasi all rights under copyright that may exist in and for the above thesis submitted for the award of the degree of “Doctor of Philosophy”.

Date: 24.10.2022

Place: Varanasi

  
(Anurag Kumar)

**Note:** However, the author may reproduce or authorize others to reproduce material extracted verbatim from the thesis or derivative of the thesis for author's personal use provided that the source and the Institute's copyright notice are indicated.

## ACKNOWLEDGEMENT

Life is a race and in today's fast-moving world, accomplishing a goal without the support of each other is a difficult task. Today, at the acme of my thesis, with heartiness, I gratefully remember many such individuals: as one flower makes no garland, this research would not have taken shape without their whole hearted encouragement and live involvement.

Foremost, I want to offer this endeavor to my almighty **Maa Saraswati** for the wisdom she bestowed upon me, the strength, peace of my mind, and good health to finish my research. We all here are very thankful to **Pandit Madan Mohan Malaviya Ji** co-founder of this institution.

I am highly indebted to my supervisor **Dr. Mohammad Imteyaz Ahmad**, Department of Ceramic Engineering, IIT (BHU), Varanasi, who inspires and encourages with his appreciating words and blessing, unflinching support, constructive criticism, truly scientific intuition, and advice exceptionally inspired me and enriched my growth as a student. My involvement with him has triggered and nourished the intellectual maturity that I will benefit for the whole of my life.

I acknowledge with thanks the kind of patronage, loving inspiration, and timely guidance, which I have received from my **RPEC members, Dr. Pradip Kumar Roy and Dr. Ashutosh Kumar Dubey and Dr. Manoj Kumar** (Department of Chemical Engineering, Varanasi) for his advice during the report evaluation each semester.

My sincere thanks to **Prof. Vinay Kumar Sing**, the Head, Department of Ceramic Engineering, IIT (BHU), Varanasi, for his kind support and for providing necessary lab facilities and a congenial working atmosphere in the Department.

I gratefully acknowledge **Central Instrumentation Facility Centre (CIFC)-IIT (BHU)**, Varanasi, for providing instrumental facilities through which I was able to perform my research smoothly and efficiently.

I also wish to thank all the **non-teaching staff** of the Department of Ceramic Engineering, Indian Institute of Technology (BHU) for their cooperation and timely help.

I would like to express gratitude to my friend **Mr. Deepak Kumar Gorai** for his help in accessing some of the characterization facilities at IIT Kharagpur. My sincere thanks also go to my fellow lab mates **Mr. Maurya Sandeep Pradeepkumar, Mr. Asim Aftab, Mr. Ashwani Gautam, Mr. Sooraj, Mr. Mukesh Suthar, Dr. Deepak Khare** from the Department of Ceramic Engineering and **Mr. Adarsh Kumar** from Department of Mechanical Engineering for their kind support and enthusiasm.

This acknowledgment would not be complete without memorizing my loving friends, from A S N Bose Hostel for their invaluable help and co-operation during my stay on campus. I appreciate their ideas, help, and good humor.

I can never forget to express my deepest thanks to all my loving family members especially bhaiya and bhabhi and beloved sisters. I would also express my eternal

appreciation towards my **parents (Shakuntala Devi and Vinod Prasad) and my uncle Suresh Prasad** who has always been there for me no matter where I am, for all his unconditional support and patience. Thank you for being so understanding and for the never-ending motivation I've been getting all this while.

Lastly, I owe my most utter gratitude to all the well-wishers who have willingly helped me out with their abilities in one way or the other.

**Anurag Kumar**

## TABLE OF CONTENTS

List of figures.....	xvi
List of tables.....	xxv
Abstract.....	xxviii
Chapter 1 .....	1
1.1 Introduction.....	1
1.2 Transparent conductive oxide (TCO) .....	3
1.3 Fundamentals of TCOs .....	3
1.3.1 Band Theory .....	4
1.3.2 Conductivity.....	5
1.3.3 Fermi level .....	6
1.3.4 Drude model of conductivity .....	6
1.3.5 Optical properties.....	8
1.4 Effect of doping on the bandgap.....	9
1.4.1 Burstein-Moss shift.....	10

1.4.2 Bandgap narrowing.....	11
1.5 ZnO-based TCO.....	12
1.6 Structural and chemical properties .....	13
1.7 Defects in ZnO.....	15
1.8 n-type dopants.....	18
1.9 Motivation.....	21
1.10 Organization of Thesis.....	22
<b>Chapter 2 Processing of Al-doped-based TCOs .....</b>	<b>25</b>
2.1 Introduction.....	25
2.2 Vapor-based deposition techniques .....	25
2.2.1 Magnetron sputtering.....	25
2.2.2 Pulse Laser Deposition .....	29
2.2.3 Chemical vapor deposition(CVD) .....	32
2.2.4 Atomic layer deposition.....	34
2.3 Solution-based processing techniques .....	35
2.3.1 AZO deposited by sol-gel dip coating/ spin coating.....	36

2.3.2 Spray pyrolysis .....	39
2.4 Post-deposition annealing .....	43
2.4.1 Vacuum annealing .....	45
2.4.2 Rapid thermal annealing/Radiative annealing .....	47
2.5 Concluding Remarks.....	48
<b>Chapter 3 .....</b>	<b>49</b>
3.1 Introduction.....	49
3.2 Preparation for deposition.....	49
3.2.1 Materials .....	49
3.2.2 Solution preparation for sol-gel spin coating.....	50
3.2.3 Solution preparation for spray coating.....	50
3.2.4 Substrate preparation for film deposition .....	50
3.3 Thin film deposition routes.....	51
3.3.1 Spin Coating .....	51
3.3.2 Spray pyrolysis .....	52
3.4 Processing of Films.....	54

3.4.1 Post deposition annealing .....	54
3.4.2 Vacuum annealing .....	54
3.4.3 Radiative annealing.....	55
3.5 Characterization Techniques.....	57
3.5.1 X-ray diffraction .....	57
3.5.2 Hall effect measurement .....	59
3.5.3 Field emission scanning electron microscope (FESEM).....	61
3.5.4 UV-VIS Spectroscopy .....	63
3.5.5 Raman spectroscopy .....	64
3.5.6 Photoluminescence .....	65
3.5.7 X-ray photoelectron spectroscopy (XPS) .....	67
3.5.8 Ultraviolet photoelectron spectroscopy (UPS) .....	70
3.5.9 Atomic Force Microscopy (AFM).....	70
Chapter 4 .....	72
4.1 Introduction.....	72
4.2 Result and Discussion.....	73

4.2.1 X-ray diffraction .....	73
4.2.2 Scanning electron microscopy .....	76
4.2.3 Scanning kelvin probe microscopy .....	78
4.2.4 Optical properties.....	80
4.2.5 X-ray photoelectron spectroscopy .....	81
4.2.6 Photoluminescence spectra .....	84
4.2.7 Electrical properties of the film .....	86
4.3 Concluding Remarks.....	89
<b>Chapter 5 .....</b>	<b>91</b>
5.1 Introduction.....	91
5.2 Result and discussion.....	92
5.2.1 X-ray diffraction .....	92
5.2.2 Scanning electron microscopy .....	95
5.2.3 Atomic force microscopy.....	97
5.2.4 Optical properties.....	100
5.2.5 X-ray photoelectron spectroscopy (XPS) .....	103

5.2.6 Ultraviolet photoelectron spectroscopy (UPS) .....	112
5.3 Electrical properties of the film .....	114
5.4 Concluding Remarks.....	118
Chapter 6 .....	119
6.1 Introduction.....	119
6.2 Result and discussion:.....	120
6.2.1 X-ray diffraction .....	120
6.2.2 Electrical properties .....	123
6.2.3 Scanning electron microscopy .....	125
6.2.4 Raman spectroscopy .....	127
6.2.5 Photoluminescence .....	130
6.2.6 X-ray photoelectron spectroscopy .....	132
6.2.7 Optical properties.....	137
6.2.8 Concluding Remarks.....	139
Chapter 7 .....	140
7.1 Introduction.....	140

7.2 Results and discussion .....	141
7.2.1 X-ray diffraction .....	141
7.2.2 Scanning Electron Microscopy .....	142
7.2.3 Optical properties.....	144
7.2.4 Electrical properties .....	145
7.2.5 X-ray photoelectron spectroscopy (XPS) .....	147
7.3 Concluding Remarks.....	152
Chapter 8 .....	153
8.1 Brief Summary and Conclusions .....	153
8.2 Suggestions for future work.....	155

## **References**

## **List of Publications**

## List of Figure

<b>Figure 1.1</b> Schematic of inter-band splitting.....	4
<b>Figure 1.2</b> Band splitting in semiconductor material with interatomic separation	5
<b>Figure 1.3</b> Drude Model.....	7
<b>Figure 1.4</b> Transmission, reflection and absorption spectra of a typical TCO [2].	9
<b>Figure 1.5</b> Optical Bandgap of semiconductor, a) Burstein Moss (BM) shifting after dopant addition, and b) Bandgap narrowing (BGN) after dopant addition c) .....	12
<b>Figure 1.6</b> Zinc oxide articles published using ZnO as a bulk material and as a thin film. (Data taken from Scopus dated 20/02/2022 using the keywords “zinc oxide” and “zinc oxide and aluminium doped zinc oxide thin films”) .....	13
<b>Figure 1.7</b> Zinc oxide polymorphs a) zinc blende, b) wurtzite, and c) rock-salt Reproduced with permission[46].Copyright 2012, Springer.....	14
<b>Figure 1.8</b> Formation energies as a function of Fermi-level position for native point defects in ZnO for (a) Zn-rich and (b) O-rich conditions (c) in presence of hydrogen[54].....	17
<b>Figure 2.1</b> Schematic diagram of RF Magnetron Sputtering.....	28
<b>Figure 2.2</b> Schematic diagram of Pulse Laser Deposition.....	31

<b>Figure 2.3</b> Schematic diagram of chemical vapor deposition.....	33
<b>Figure 2.4</b> Available solution-based deposition techniques used for precursor solution deposition with the help of proper solvent. Reproduced with permission [183]. Copyright 2011, Royal Society Of Chemistry .....	36
<b>Figure 2.5</b> Schematic of the spray pyrolysis deposition procedure .....	39
<b>Figure 2.6</b> Stages during spray pyrolysis process .....	41
<b>Figure 2.7</b> Schematic of the competition between deposition and evaporation rate on crystallization.....	41
<b>Figure 3.1</b> Schematic flow diagram of ZnO and AZO film deposition with the spin coating setup .....	52
<b>Figure 3.2</b> Pictorial diagram of thin film deposition of ZnO , AZO, TZO, and TAZO by spray pyrolysis .....	53
<b>Figure 3.3</b> (a) Photograph of the tubular furnace, (b) schematic of the defect reaction occurring during vacuum annealing, and (c) temperature profile for the vacuum annealing .....	55
<b>Figure 3.4</b> (a) Schematic of radiative annealing setup, (b) Photograph of radiative annealing setup, (c) Temperature profile for the radiative annealing .....	56
<b>Figure 3.5</b> Schematic diagram of Bragg's law.....	57

<b>Figure 3.6</b> a) Photograph of bench top XRD image, b) Photograph of the front view of GIXRD, and c) Enhanced view of GIXRD sample stage .....	59
<b>Figure 3.7</b> a) Schematic of Hall effect measurement b) Photograph of Hall Effect Measurement system setup and, c) Sample with silver contact d) Photograph of the sample holder.....	60
<b>Figure 3.8</b> a) Front view of FESEM b) Side view of FESEM.....	62
<b>Figure 3.9</b> a) Photograph of UV VIS spectroscopy setup and, b) Photograph of the sample holder chamber .....	63
<b>Figure 3.10</b> Schematic of working of Raman spectroscopy .....	64
<b>Figure 3.11</b> Jablonski diagram of fluorescence and phosphorescence processes and their typical rate constants .....	66
<b>Figure 3.12</b> a) Pictorial representation of major components of XPS b) Photograph of the X-ray photoelectron spectroscopy .....	67
<b>Figure 3.13</b> a) Diagram of Auger electron emission, and b) Auger electron emission in X-ray notation ( $KL_1L_{2,3}$ ).....	69
<b>Figure 3.14</b> Ultraviolet photoelectron spectroscopy spectrum for reference.....	70
<b>Figure 3.15</b> a) Pictorial representation of AFM b) Photograph of atomic force microscope .....	71
<b>Figure 4.1</b> XRD pattern of pure ZnO and 1-3 at% Al-doped ZnO .....	75

<b>Figure 4.2</b> Crystalline size and strain as a function of Al doping concentration from 0 to 3 at.% .....	77
<b>Figure 4.3</b> SEM images of ZnO doped with a) Pure ZnO b) 1 at.% Al c) 2 at.% Al d) 3 at.% Al.....	77
<b>Figure 4.4</b> Two-dimensional a) contact potential difference $V_{CPD}$ image of 2 at. % Al-doped ZnO b) 2D image of surface roughness of 2 at. % Al-doped ZnO.....	79
<b>Figure 4.5</b> Transmittance a) absorbance and Tauc plot (inset) b) of Al-doped ZnO films having ZnO and 1 to 3 at. % Al concentration .....	81
<b>Figure 4.6</b> Scanned peaks and fitted shoulder peaks on higher binding energy side (a) Zn2p and, (b) Zn 2p <sub>3/2</sub> orbitals .....	83
<b>Figure 4.7</b> Wide scan XPS spectrum of Al 2p core level AZO thin film doped with 1 at% Al .....	83
<b>Figure 4.8</b> Photoluminescence spectra of a) undoped ZnO and 1-3 at% Al-doped zinc oxide b) deconvoluted peaks of zinc oxide thin film (Inset: Energy band diagram based on deconvoluted peaks) .....	84
<b>Figure 4.9</b> PL peak intensity normalized to the band edge PL intensity as a function of Al concentration .....	86
<b>Figure 4.10</b> Electrical properties of undoped and 1-3 at% Al-doped zinc oxide..	88

<b>Figure 5.1</b> X-ray diffraction pattern of undoped and 1AZO as-deposited and vacuum-annealed film.....	94
<b>Figure 5.2</b> HR SEM images of a) Pure ZnO film, b) 1AZO films, c) cross-sectional view of pure ZnO films, d) cross-sectional view of 1AZO films, e) ZnO film after vacuum annealing, and f) 1AZO film after vacuum annealing .....	96
<b>Figure 5.3</b> Surface topography images of as-deposited(a) ZnO, (b) 1AZO film and vacuum annealed, (c) ZnO, and (d) 1AZO film .....	98
<b>Figure 5.4</b> Roughness and waviness profile of a) as deposited ZnO b) as deposited 1AZO c) vacuum annealed ZnO d) vacuum annealed 1AZO thin film.....	99
<b>Figure 5.5</b> a) & c) Transmittance as a function of wavelength of ZnO and 1AZO of as-deposited and vacuum annealed thin film respectively, b) & d) absorbance plot of ZnO and 1AZO thin film (inset shows the Tauc plot) of as-deposited and vacuum annealed, respectively .....	101
<b>Figure 5.6</b> Photoluminescence of zinc oxide and 1AZO thin film as deposited and vacuum annealed.....	102
<b>Figure 5.7</b> a) A fitted PL spectrum of 1AZO films, and b) Normalized intensity of PL peaks from defect level .....	103
<b>Figure 5.8</b> XPS of O1s orbital of ZnO and 1AZO films in as-deposited and vacuum-annealed condition .....	106

<b>Figure 5.9</b> XPS of O1s orbital of a) as deposited ZnO, b) ZnO vacuum annealed, c) as deposited 1AZO, and d) vacuum annealed 1AZO .....	106
<b>Figure 5.10</b> XPS of Zn2p orbital undoped and 1AZO thin film in as-deposited and vacuum annealed condition .....	108
<b>Figure 5.11</b> Comparative XPS of Zn2p <sub>3/2</sub> orbital of as-deposited and vacuum-annealed ZnO and 1AZO film .....	108
<b>Figure 5.12</b> X-ray photoelectron spectroscopy of Al2p orbital 1AZO as-deposited and vacuum annealed.....	109
<b>Figure 5.13</b> Valence band XPS of Zn 3d orbital of zinc oxide thin film a) pure ZnO and b) 1AZO films .....	109
<b>Figure 5.14</b> (a) High energy cut-off, and (b) valence band onset of UPS spectra recorded for pure ZnO and 1AZO films in as-deposited and vacuum annealed condition .....	111
<b>Figure 5.15</b> Energy level band diagram of zinc oxide thin film a) pure ZnO as-deposited b) vacuum annealed doped ZnO as-deposited c) 1AZO thin film as deposited d) 1AZO thin film vacuum annealed.....	114
<b>Figure 6.1</b> X-ray diffraction pattern a) as-deposited and b) radiative annealed pure ZnO and 1-3 at% Al-doped ZnO (AZO) films .....	121
<b>Figure 6.2</b> Lattice parameter of as-deposited and radiative annealed pure ZnO and 1-3AZO films.....	122

<b>Figure 6.3</b> Resistivity a) bulk carrier concentration and mobility b) of as-deposited and radiative annealed pure zinc oxide and 1-3AZO thin films .....	124
<b>Figure 6.4</b> As deposited film of a) ZnO b) 1AZO c) 2AZO d) 3AZO .....	125
<b>Figure 6.5</b> Radiative annealed film a) ZnO b) 1AZO c) 2AZO d) 3AZO .....	126
<b>Figure 6.6</b> SEM images of a) cross-sectional view of as-deposited 2AZO thin film, and d) cross-sectional view of 2AZO thin film after radiative annealing .....	126
<b>Figure 6.7</b> Raman spectroscopy of as-deposited and radiative annealed ZnO, 2AZO, and 3AZO films .....	128
<b>Figure 6.8</b> As deposited and radiative annealed deconvoluted $A_1(LO)$ peak of ZnO .....	129
<b>Figure 6.9</b> Raman spectrum of 2AZO as-deposited and radiative annealed.....	129
<b>Figure 6.10</b> a) PL spectra of as-deposited and radiative annealed pure ZnO and 2-3AZO, and b) deconvoluted peaks of radiative annealed 2AZO .....	130
<b>Figure 6.11</b> XPS of O1s orbital of a) ZnO as deposited b) ZnO radiatively annealed c) 2AZO as deposited d) 2AZO radiative annealed .....	133
<b>Figure 6.12</b> XPS of Zn2p orbital pure ZnO a) and 2AZO thin film b) as-deposited and radiative annealed .....	134
<b>Figure 6.13</b> X-ray photoelectron spectroscopy of Al2p orbital a) 2AZO as deposited b) 2AZO after radiative annealing.....	136

<b>Figure 6.14</b> Valence band XPS of Zn3d orbital of a) pure ZnO, and b) 2AZO films as deposited and radiative annealed.....	136
<b>Figure 6.15</b> a) As deposited, and b) radiative annealed transmittance of the pure ZnO and 1-3AZO films.....	137
<b>Figure 6.16</b> a) As deposited, and b) radiative annealed absorbance and Tauc plot (inset) of the pure ZnO and 1-3AZO films .....	138
<b>Figure 6.17</b> Figure of merit of as-deposited and radiative annealed pure ZnO and 1-3AZO thin films .....	139
<b>Figure 7.1</b> X-ray diffraction pattern of TZO, TZHO, TAZO, and TAZHO films .....	142
<b>Figure 7.2</b> Scanning electron microscopy images of as-deposited and radiative annealed (a) TZO, (b) TZHO, (c) TAZO, and (d) TAZHO films, (inset in each image shows the cross-section).....	143
<b>Figure 7.3</b> a) Transmittance b) absorbance and Tauc plot in (inset) of TZO and TAZO of as-deposited and radiative annealed thin films .....	144
<b>Figure 7.4</b> a) Resistivity of the films b) shows the mobility( $\mu$ ) c) shows the bulk carrier concentration (n) as a function of the temperature of TZO, TZHO, TAZO, and TAZHO films.....	146
<b>Figure 7.5</b> Interaction of s-s orbital for heavy metal cations and light metal cations .....	147

<b>Figure 7.6</b> XPS of TAZO a) TAZHO O1s orbital b) XPS of TAZO c) TAZHO Al2p orbital .....	149
<b>Figure 7.7</b> Auger peaks of (ZnLMM) of as-deposited (a) TAZO and, (b) annealed TAZHO films.....	151

## List of Table

<b>Table 1.1</b> ZnO polymorph space group, lattice constant, bond energy and formation energy.....	14
<b>Table 2.1</b> Electrical and optical properties achieved by various researchers on AZO films deposited using RF/DC magnetron sputtering technique .....	29
<b>Table 2.2</b> Doping percentage, thickness, substrate/annealing temperature, resistivity, charge concentration, mobility, and %T values reported in various scientific studies on AZO films deposited using PLD technique .....	31
<b>Table 2.3</b> Doping percentage, thickness, substrate/annealing temperature, resistivity, charge concentration, mobility, and %Transmittance values reported in various studies on AZO films deposited using a chemical vapor deposition technique.....	33
<b>Table 2.4</b> Characteristics of Atomisers Commonly Used for spray pyrolysis [190] .....	39
<b>Table 2.5</b> Doping percentage, thickness, substrate/annealing temperature, resistivity, charge concentration, mobility, and %T values reported in earlier studies on AZO films deposited using spray pyrolysis technique .....	43
<b>Table 4.1</b> XRD peak intensity of zinc oxide and Al-doped ZnO films normalized relative to (101) and compared to zinc oxide random powder XRD peak intensity ratio .....	76

<b>Table 4.2</b> Crystalline size and grain size of wurtzite structure planes of (0-3) at.% Al-doped ZnO .....	78
<b>Table 4.3</b> Bandgap of ZnO and 1 to 3 at.% Al-doped zinc oxide films.....	81
<b>Table 5.1</b> Lattice parameters (a and c), crystallite size, and texture co-efficient ( $T_C$ ) of the pure ZnO film, 1AZO films, and ZnO bulk reference. ZnO bulk reference data adapted from the database (JCPDS number:00-003-0888).....	95
<b>Table 5.2</b> Roughness parameters of as-deposited and vacuum-annealed ZnO and 1AZO thin films.....	100
<b>Table 5.3</b> The trend of $V_o/O_{Lat}$ and $O_{Ads}/O_{Lat}$ in XPS spectra of O1s pure ZnO and 1AZO films as-deposited and vacuum annealed .....	107
<b>Table 5.4</b> Electronic and optical properties of ZnO and 1AZO thin films .....	112
<b>Table 5.5</b> Electrical properties of Al-doped and undoped zinc oxide films, as-deposited and vacuum annealed .....	116
<b>Table 5.6</b> Figure of merit ( $F_{TC}$ ) and deposition temperature of pure and Al-doped zinc oxide films prepared by solution processing.....	117
<b>Table 6.1</b> Raman spectra and peak location in case of as-deposited and radiative annealed ZnO, 2AZO, and 3AZO thin films .....	128
<b>Table 6.2</b> Defect energy location in as-deposited and radiative annealed ZnO, 2AZO, 3AZO thin films.....	131

<b>Table 6.3</b> $O_{\text{Ads}}/O_{\text{Lat}}$ and $O_{\text{Def}}/O_{\text{Lat}}$ obtained from deconvoluted O1s XPS peak of pure ZnO and 2AZO films as deposited and radiative annealed .....	134
<b>Table 7.1</b> Centre of gravity (COG), FWHM, Crystalline size (nm), d-spacing, lattice parameter ( $c$ ), of TZO, TZHO, TAZO and TAZHO .....	142
<b>Table 7.2</b> Trend of $O_{\text{Ads}}/O_{\text{Lat}}$ and $O_{\text{Vac}}/O_{\text{Lattice}}$ TAZO and TAZHO thin film.....	150

## Abstract

Good electrical conductivity, high chemical stability in harsh environments, and transparency in the visible range make transparent conductive oxides (TCOs) suitable for numerous applications in optoelectronic devices. Indium-tin oxide (ITO) is the most widely used TCO due to its high transmittance in the visible region and low resistivity. However, the shortage of indium resources, toxicity, and cost are a cause of concern for the fast-growing optoelectronic device industry. Owing to the increasing demand, higher cost, and limited availability of In, alternatives for the ITO with comparable properties and low cost are being sought. Over the last decade, ZnO-based TCOs have emerged as a possible earth-abundant, non-toxic replacement for ITO for many optoelectronic applications. ZnO films have high chemical and thermal stability and a higher bandgap ( $\sim 3.3\text{-}3.6$  eV), ensuring transparency in the visible regime. Out of the available choice of dopants, Al is earth-abundant and has ionic radii close to that of Zn, making it the dopant of choice. Although various methods can be utilized to deposit ZnO films, low resistivity ( $\sim 10^{-4}$   $\Omega\text{-cm}$ ) and high transparency ( $>85\%$ ) have traditionally been achieved by sputtering/PLD mainly because of good crystallinity and orientation, which enhances carrier mobility. However, the installation and processing cost of sputtering or PLD is high and not easily scalable. On the other hand, solution-based processing techniques are much cheaper and simpler and at the same time, easily scalable. However, AZO films processed through the solution route generally result in lower resistivity values. A straightforward way to increase the electrical conductivity while maintaining the optical transparency is to increase the carrier

concentration, passivate the defect and grain boundaries and enhance mobility. However, carrier concentration can be helpful up to a certain extent. A high concentration (generally  $>10^{20} \text{ cm}^{-3}$ ) in ZnO-based TCOs results in greater scattering and reduced mobility. The main objective of this work is to improve the performance of solution-processed ZnO-based TCO at par with that of sputtered films.

Initially, Al-doped ZnO films were deposited on glass substrates by the sol-gel spin coating route. The formation of the wurtzite structure was confirmed by the x-ray diffraction (XRD) pattern; however, the films were not oriented. Transparency of about 85% was obtained in visible and near IR regimes as examined by UV-Vis spectroscopy. The bandgap increased from 3.14 to 3.19 eV on increasing Al concentration from 0 to 3 at.%. The obtained resistivity was in the order of  $10^{-2} \Omega\text{-cm}$  while charge concentration and mobility were  $\sim 10^{19} \text{ cm}^{-3}$  and  $\sim 15 \text{ cm}^2/\text{Vs}$ , respectively. Photoluminescence of Al-doped zinc oxide thin film indicated the presence of Zn interstitials. The carrier concentration increased up to 2 at% Al doping while greater doping resulted in a reduction in carrier concentration, which was attributed to the formation of greater amounts of  $\text{Al}_2\text{O}_3$  at the grain boundaries. Both scanning Kelvin probe microscopy and photoluminescence confirmed the presence of defects localization at grain boundaries.

To improve film orientation, increase carrier concentration and achieve a better surface finish, spray pyrolysis was utilized for deposition. The deposited films were vacuum annealed for twenty minutes. Electrical, optical, morphological, and surface-specific properties of zinc oxide and aluminum doped zinc oxide thin film

was investigated. The effect of oxygen vacancies on the Fermi level and conductivity of the films were analyzed. The Fermi level was at 3.21 and 3.31 eV for the pure and 1 at% Al-doped films (1AZO), which on vacuum annealing, increased to 3.27 and 3.4 eV, respectively. The work function of the as-deposited zinc oxide and 1AZO films were 5.65 and 4.38 eV, which on vacuum annealing decreased to 4.05 eV and 4.04 eV, respectively. A carrier concentration as high as  $\sim 1.77 \times 10^{20} \text{ cm}^{-3}$  with mobility of  $\sim 50 \text{ cm}^2/\text{Vs}$  and resistivity close to  $\sim 2 \times 10^{-3} \text{ } \Omega\text{-cm}$  was achieved for 1 at. % Al-doped ZnO (1AZO) film. Transparency greater than  $\sim 82\%$  and a figure of merit 1.14 was achieved, which is one of the best-reported values for solution-processed AZO films. Although the film met the critical requirement, transparency of the film was on the lower side. At the same, it involved vacuum annealing for defect generation, which had concerns about stability.

In order to enhance the performance and stability and reduce the thermal budget, the spray-deposited films were radiatively annealed (10 s at 480 °C) in a 5% $\text{H}_2$  + Ar atmosphere. Fast radiative annealing improved the mobility while increasing the carrier concentration by as much as 10 times when compared with as-deposited films. Resistivity as low as  $\sim 2 \times 10^{-3} \text{ } \Omega\text{-cm}$  with  $\sim 94\%$  transparency at 550 nm wavelength for 2% Al-doped ZnO (2AZO) films was achieved. PL and Raman spectroscopy revealed that the hydrogen passivated the defects ( $\text{Zn}_i$  and  $\text{V}_O$ ) and grain boundaries resulting in improved mobility and transparency. XPS and UV visible spectroscopy revealed activation of greater amounts of Al dopants at the same time, passivating  $\text{V}_O$  by partial  $\text{H}^+$  substitution, increased carrier concentration, and wider optical bandgaps.

To further minimize the resistivity of radiative annealed 2AZO film, thallium (Tl) was introduced as a co-dopant. Scanning electron microscopy images showed columnar grain growth in Tl-Al co-doped ZnO. The transparency of the film further improved after co-doping to ~92%, while the resistivity of the film was  $\sim 9 \times 10^{-4} \Omega\text{-cm}$ . Charge concentration increased to  $\sim 2.4 \times 10^{20} \text{ cm}^{-3}$  while the mobility was  $\sim 56 \text{ cm}^2/\text{Vs}$ . High mobility was attributed to the lower electron effective mass in the presence of thallium due to greater s orbital overlap, while the presence of Tl also increased the carrier concentration.